Optical Supplemental Navigation Device (OSN)

Wilfredo Ortiz, Joseph Devenport, Cedric Harper, Henry Schmitz

Dept. of Electrical Engineering and Computer Science, University of Central Florida, Orlando, Florida, 32816-2450

***Abstract* — An affordable navigation system for the visually impaired based on LIDAR technology was designed using the Time-of-Flight (ToF) principal. A nanosecond pulsed laser was employed along with a receiver and timing circuit. The device provides feedback to the user that coincides with the distance that it measures. This allows the user to gain more information about their surroundings than a white stick.**

***Index Terms* — Laser rangefinder, Light detection and ranging (LIDAR), photodiode receiver, pulsed laser diode, Time-to-Digital Converter (TDC), MOSFET driver, haptic feedback.**

I. Introduction

The cane stands as the all around best technology for the visually impaired. This has been the case around the world for thousands of years. In 1921, the cane was first upgraded to be solely white. The main benefit for this standardization was alerting motorists that the individual using the cane was visually impaired. Since then the white cane has become a universal symbol for the visually impaired [8]. Also, since then not many upgrades have been made for the visually impaired to help them maneuver in today's faster-paced society. This group's objective is to make a difference by using current advancements in technology to improve upon the time-tested white cane. LIDAR technology was chosen to accomplish this.

Using a laser rangefinder as a supplement to the white cane allows for greater range in distance for user feedback. While the white cane currently gives feedback to a distance of about 1 meter, the addition of this laser rangefinder should allow detection of objects from 1 meter up to 4 meters from the user. This will increase confidence and speed of the visually impaired when maneuvering through unknown environments. There are other products currently providing this service using ultrasonic technology. The main problem with these products is they are too expensive for the average visually impaired person. LIDAR technology was selected to provide better accuracy and a much-needed lower cost for the user.

II. Design

The three major components of the system are the transmitter, receiver, and timing module. Figure 1 below shows a general flow diagram containing each of the major components of the overall design.

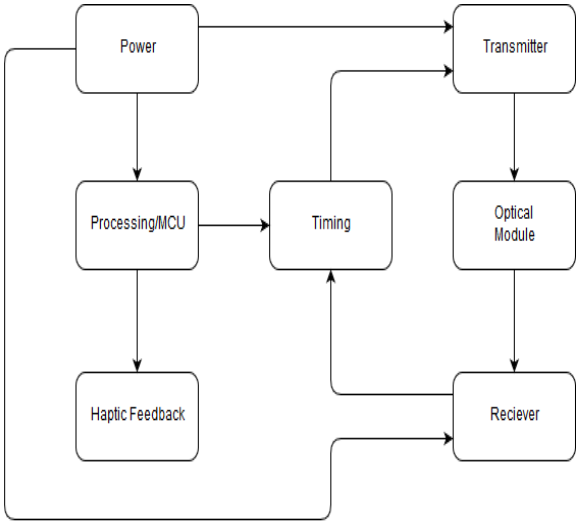

Figure 1: System flow diagram

A. *Transmitter*

The Ti UCC37322 CMOS laser driver (Figure 2) meets the pulsed laser's demands of requiring a high pulse trigger current in order to meet the inherent 5V threshold fixed by the laser's internal MOSFET [1]. VG1 (the input voltage to the left in the driver schematic) is the TTL-level signal supplied by our microcontroller at an upper level of about 5V and a frequency of 1 kHz. TTL stands for Transistor-Transistor Logic and plays a vital role in this device overall [2]-[3]. Operating at this frequency offers several advantages: allows us to obtain shorter electrical pulses (around 125ns) given limitations on duty cycle set by our low speed microcontroller, offers greater ease in filtering out high frequencies, and should simplify integrating timing tasks overall.

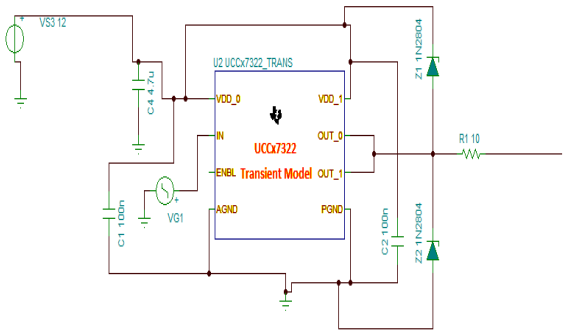

Figure 2: High speed laser driver schematic

This project makes use of the OSRAM SPL LL90 laser diode (Figure 3) that emits a wavelength around 910nm (Near IR) when supplied with a charge voltage (12V in our case), a TTL signal (coming from the CMOS laser driver), and properly grounded. This multi quantum well (MQW) [4] semiconductor laser comes equipped with a small amount of built-in circuitry that includes a MOSFET, a laser chip, and a few capacitors. These capacitors for the most part restrict the maximum laser pulse width to around 40ns. This pulse width in turn has an effect on the overall duty cycle. The duty cycle for this laser should not exceed the recommended maximum of 0.1%. In the case of this project, this duty cycle is not of concern considering that the selected pulse frequency is only 1kHz (well within 25kHz).

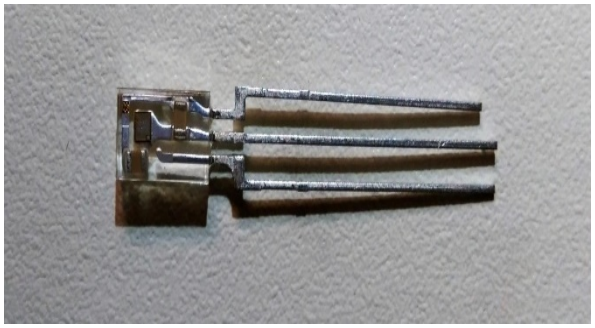

Figure 3: OSRAM pulsed laser diode

B. *Receiver*

The receiver consists of three major components: the KBX139AR.16 50.8 mm diameter lens with antireflective coating for 650 nm to 1000 nm wavelengths, the SFH 2701 PIN photodiode, and the OPA380 operational amplifier.

High speed components are necessary for this application. At the cost, the SFH 2701 photodiode is hard to beat. It boasts a 1.8 ns rise time with an effective area of .36 mm^2, adding less junction capacitance than a larger area photodiode, and thus, keeping the speed high. In addition to the specifications, reverse biasing the photodiode keeps it operating at its maximum speed.

Since the photodiode is operating in photoconductive mode, the OPA380 transimpedance amplifier was employed in order to convert the photocurrent into a useable voltage to trigger the TDC to stop. Since the TDC requires a minimum of 2 V to trigger a start or stop, supplying the op amp with 5 V and adding a 10K ohm feedback resistor allows for sufficient amplification for the TDC to function properly.

C. *Optical Module*

In order to test the receiver and the transmitter, it was necessary to create components to facilitate alignment of the optics. By taking the specifications of the SBX013AR.16 and KBX139AR.16 lenses, the laser diode, and the effective area of the photodiode, an optical module was then designed using simple geometrical optics. Factors such as lens thickness, Back Focal Length (BFL), and Effective Focal Length (EFL) specifically were considered and an appropriate model designed accordingly. The Solidworks figure (Figure 4) shows a side view of the transmitter module. The figure depicted below of the transmitter is an exploded view of the receiver module (figure 5). Both were designed specifically to fit the SPL LL90 pulsed laser diode and the SFH 2701 PIN photodiode, respectively. The modules are adjustable in order to find the best focal point for both sides.

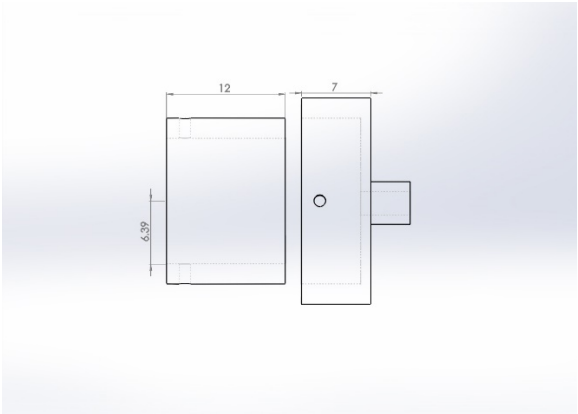

Figure 4: Side view of the transmitter module highlighting the total amount it could be adjusted axially (18 mm) and the radius of the aperture housing the KBX022 lens

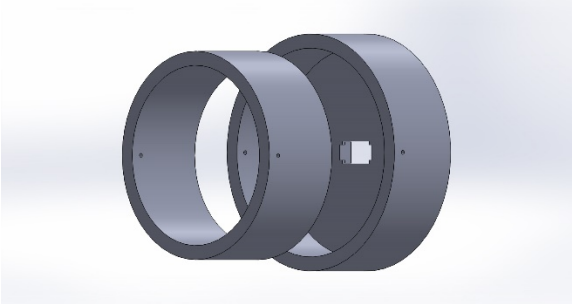

Figure 5: Side view of the receiver module. The opening on the backside houses the PIN photodiode

The transmitter side on the project uses the Newport SBX013 bi-convex fused silica lens (in Figure 6 below). Of course, this type of lens is more in terms of material than is needed (fused silica is typically used in high power applications). This lens was donated to UCF and readily available. Besides being easily obtainable, this lens has a short focal length (12.6735mm) and a AR coating directly suitable for our laser's wavelength. The main issue in finding the best lens for this device is that the semiconductor laser's output is highly divergent [1]. One might account for this divergence with an expensive custom optic that reduces spherical as well as other higher-order aberrations. Another method might be accommodation via a properly placed cylindrical lens that only alters the beam's fast axis before collimation.

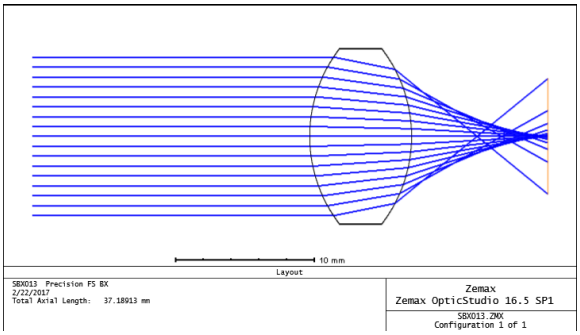

Figure 6: 2D Zemax layout of Newport SBX013

The receiver side uses the KBX139AR.16 lens. The diameter of the lens allows for maximum collection of light to be focused onto the detector out of all of the lenses that were tested. This lens also has an antireflective coating that works well for the wavelength of the laser diode and allows for minimum noise to be introduced due to ambient light. Figure 7 shows a Zemax rendition of the lens.

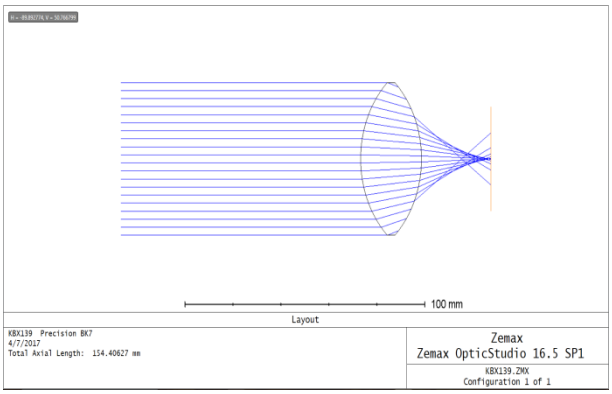

Figure 7. 2D Zemax layout of Newport KBX139

D. Timing Module/Microcontroller

The most crucial part of the overall design is the ability to measure the time it takes for the laser to leave the transmitter and the receiver to detect the signal. This measurement is accomplished using Texas Instrument's TDC7200. This chip was initially designed as a digital counter and is used in many applications that utilize time of flight. Figure 8 below shows a conceptual diagram of the basic operation of the timer. The timer takes measurements by creating a timestamp at the initial pulse of the laser. Once that pulse is received by the timing module, a second timestamp is recorded. Subsequent timestamps for the receiver are created (depending on how many are desired) according to what is programmed.

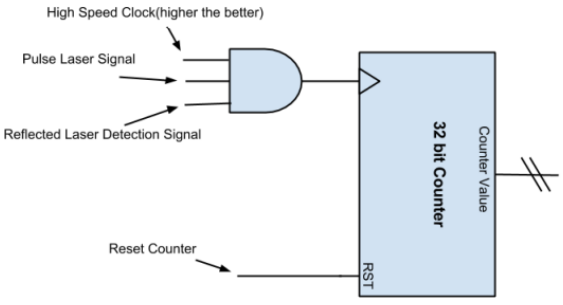

Figure 8: TDC7200 timing functionality

There are two measurement modes that the timer is capable of. The first measurement mode is capable of measuring times between 12ns and 500ns. The second measurement mode is able to measure between 250ns and 8ms. The first measurement mode will be ideal for the application, as detecting objects within short distances satisfy the objectives of this particular rangefinder.

In order to accomplish such a feat, the microcontroller communicates to the device via SPI, initially configuring the registers of the TDC to operate to our specifications. Once the registers are configured, the start/stop measurements are taken by the TDC and recorded in TIME_X registers. The amount of measurements desired is what determines 'X'. An external clock of 8 or 16 MHz is required to ensure a low standard deviation. The TDC allows for a 55ps resolution with a standard deviation of 35ps.

E. Haptic Feedback

Haptic feedback was chosen over an auditory response such as a beep In order for the user to sense how far away an object is. This decision was made based on advice given by the advisors at the Rehabilitation Center for the Blind and Visually Impaired out of Daytona Beach, FL. The main reason for this is that a visually impaired person's hearing is so vital when navigating. They are constantly listening to their environment for possible cautionary feedback, such as vehicles driving down the street. Having a beeping response from a rangefinder could possibly take away from this.

Figure 9: ERM coin motor

When deciding on the type of motor to choose eccentric rotating mass vibration motors (ERM) and linear resonant actuators (LRA) were both considered [9]. Looking at different variations of each the final choice was a 'pancake' design ERM DC motor. The main reason for this was the low profile it provides which helps to keep from adding unwanted size to the final product. If the vibration from a single motor is not sufficient, they are small enough that two could be included in the design. The dimension for one is 10mm x 2.7mm, with a weight of 0.2 ounces. The vibration of one is strong enough to alert the user when needed. The motors purchased offer 0.1A when providing 3V and 0.05A at 1.5V. The vibrations will be controlled by the microcontroller. There will be four different levels of feedback changing at each meter from 4 meter to 1 meter away. At 4 meters the frequency of the motor will vibrate slow and it will vibrate faster at each subsequent meter until it reaches the fastest vibration at one 1 meter.

III. POWER MANAGEMENT

Although there are endless choices when considering methods for powering the device, size was near the top in priority. Because of this size limitation, a battery of reasonably small size and proper voltage would prove to be necessary.

Another major component of the power module would be proper distribution of the power across multiple devices. Due to the number of components required, a critical part of the design required regulating the voltages to ensure safe operation of all electrical components. Most of the IC's and microcontrollers involved require different voltages in order to operate within the proper parameters. The three values used most are 9V, 5V, and 3.3V. In order to cater to this demand, three voltage regulators are used which outputs the three respected voltages. Similar schematics were used for each of the voltage regulator circuits (these are displayed in Figure 10 below).

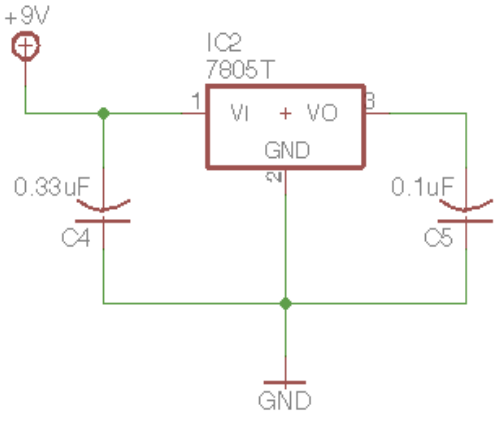

Figure 10: Voltage regulator circuit

V. TESTING

A. Transmitter

Testing the transmitter was only feasible after proper pulsing with the CMOS driver became a reality. Once that was accomplished (as briefly described in the laser driver portion of this paper), the output beam was made incident onto a spectrum analyzer. Following spectrum analysis, it was determined that the laser's peak emission was in the vicinity of 910nm (the spectrum analysis data is shown in the following section as Figure 11). This came as a surprise considering that the laser purchased was reported to be closer to 850nm. Although this meant that the transmitter was still Near IR, our optical band pass filter was rendered useless (it is very narrow). Thankfully, this offset is largely compensated by the antireflection coating on the receiver lens that should filter out most visible light and below the visible spectrum.

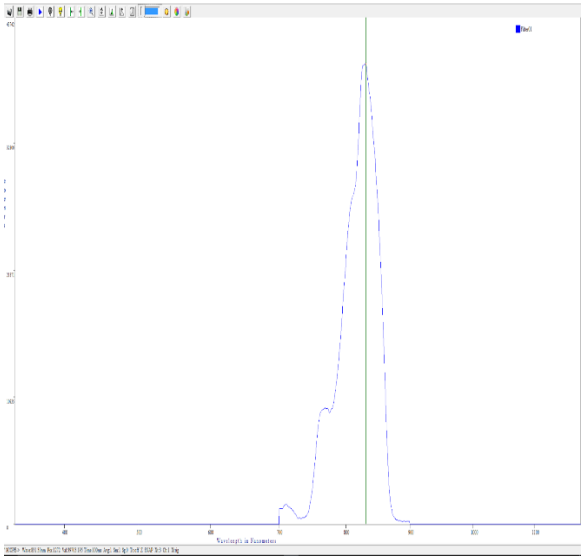

Figure 11: Laser spectrum

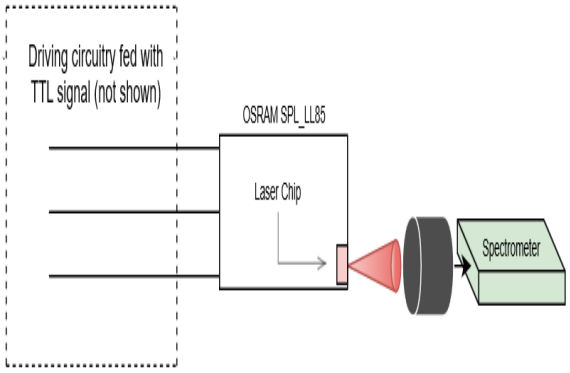

Figure 12: Testing setup for measuring optical spectrum

B. Receiver

Testing of the receiver was performed after acquiring the desired photodiode and op amp. The photodiode was reverse biased to operate in photoconductive mode and the op amp was connected in the configuration shown in figure 13. It was verified that the voltage measured at the output of the op amp was dictated by the amount of light incident on the photodiode.

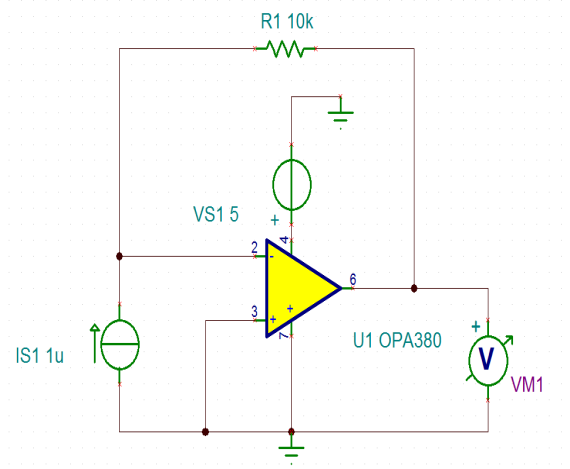

Figure 13: Transimpedance amplifier circuit

C. Signal Detection

The figure below (Figure 14) shows the initial TTL signal (in blue) and the signal received (open air) following amplification (in yellow). This successful detection marks a milestone that played a part in motivating this projects completion. Notice that the overall time delay (around 181.9ns) still

allows for time-of-flight detection using the TDC because it places the detected signal (coming from around 1m away) within the device's measurement mode 1 window (12ns-500ns). The manufacturer boasts of a 55ps resolution within this window [4].

Figure 14: Output / Input electrical signal.

D. Timing Module/Microcontroller

Initial testing for the TDC7200 consisted of using the microcontroller to write to registers, then read those registers back to ensure that proper communication was being established between the two. Next, signals were generated with the function generator and connected to the START and STOP pins of the IC. Two test were taken with two different delays to test both measurement modes.

E. Power Module

Testing for the power module included connecting the 12V battery to the input of the 9V regulator, whose output connected to the input of the 5V regulator, and whose output connected to the 3.3V regulator. Each of the outputs were measured using a digital multimeter to ensure that the proper voltages were shown at each of the outputs. Next, the individual components were connected to ensure that they were properly powered.

F. Haptic Feedback

The vibration coin ERM motors were tested with the msp430 microcontroller. A voltage divider circuit must be properly implemented to supply a voltage of 3V to the motor. The microcontroller code's delay should be adjusted according to any frequency variations and should account for a general change in distance. Ideally, different frequency ranges can be set in order to offer a more integrative rather than jitter-filled response. If using an Arduino to obtain the desired current draw, then the 5V pin is used. This allows for sending the optimal voltage with an n or p-channel MOSFET. In addition, motor must be set in parallel with a Schottky Diode and a capacitor [6].

G. System Testing

The testing of the system as a whole started with the power, transmitter, and receiver sections set up on breadboards. The TDC7200 was not yet used in the initial testing setup. A TDC7200 evaluation model (TDCEVM) was used making sure the timing was as accurate as possible in the beginning stages.

With a DC power source providing power to each component necessary, an msp430 was used to pulse the laser. To monitor the signals two oscilloscope probes were used. One to monitor the laser transmitter and one set on the transimpedance amplifier showing the signal from the photodiode. These two waveforms gave the time-response waveforms on the oscilloscope. The TDCEVM was used as the stopwatch to time the transmitted signal and the received signal. It was connected to a computer GUI which displayed the time in nanoseconds along with the standard deviation. The TDCEVM's start pin was connected to the laser transmitter, while the stop pin was connected to the transimpedance amplifier. The TDCEVM provided quick feedback to allow adjustment of the setup and obtain the intended results. There was a delay of around 175ns in the system from the signal to the laser driver to the time the laser actually lased. Because of this, each time obtained for 1-4 meters fit in the time window Measurement Mode 1 on the TDC7200.

Getting the return signal from a mirror was the first surface tested. The mirror provided the sharpest rise time and cleanest return pulse. This helped to confirm proper TDC setup. However, it was noticed that changing the angle created a walk error in the

signal. That is, the calculated time would change with the received signal's amplitude. Considering that operations are performed where nanoseconds count, this error will result in a big change reflected by inaccurate timing. This problem was somewhat improved by manually controlling the incident angle and by taking TDC stop measurements directly after the first receiver amplifier. After using a mirror, non-reflective surfaces were tested with some success at first using the Newport SBX013 lens before the photodiode. After adjusting the circuit the original smaller lens was producing the same results. Because of this we may use the smaller lens in the end. The received signal did not always produce enough voltage following the first op amp (the TDC required at least 2 volts for a stop) so additional components such as a comparator was considered. Testing from 1 to 4 meters was finally returning a pulse strong enough to trigger the TDC.

VI. CONCLUSION

The major problem to overcome looking forward is the timing walk error. The walk error may be accounted for by implementing Automatic Gain Control into the circuit. The purpose for this is to standardize the amplitude so that the timing changes become a function of distance and not the intensity of the return signal.

Designing, testing, and building this rangefinder proved to be one of the most challenging projects the participants have encountered. Most technologies involved in similar applications utilize a pre-built rangefinder. Because one of our main goals involved cost-efficiency, we concluded that the only way to accomplish this objective was to design our own. We believe that our application of this technology will prove to be most beneficial to the visually impaired. We hope to continue development of this project so that one day our idea might help thousands of visually-impaired people across the globe.

ACKNOWLEDGEMENTS

We wish to thank the faculty and staff at UCF and CREOL who have helped guide and support our project. We would also like to thank Lockheed Martin and Newport for their support.

REFERENCES

[1] Morgott/OSRAM, S. (2004, November 3). Operating the Pulsed Laser Diode SPL LLxx [Application Note].

[2] ^ Eren, H. (2003), Electronic Portable Instruments: Design and Applications, CRC Press, ISBN 0-8493-1998-6

[3] "Transistor–transistor logic," Wikipedia. [Online]. Available: https://en.wikipedia.org/wiki/Transistor–transistor_logic. [Accessed: 02-Dec-2016].

[4] S. O. Kasap, Optoelectronics and Photonics, 2nd ed. Upper Saddle River, New Jersey: Pearson Education, 2013.

[5] "Low-cost LIDAR – a key technology to enable autonomous driving in urban environments," *Low-cost LIDAR – a key technology to enable autonomous driving in urban environments | OSRAM Opto Semiconductors*, 03-Jun-2015. [Online]. Available: http://www.osram-os.com/osram_os/en/press/press-releases/ir-devices-and-laser-diodes/2015/low-cost-lidar--a-key-technology-to-enable-autonomous-driving-in-urban-environments/index.jsp?search_result=%2Fosram_os%2Fen%2Fpress%2Fpress-releases%2Findex.jsp%3Faction%3Ddosearch. [Accessed: 07-Apr-2017].

[6] "How to Drive a Vibration Motor with Arduino and Genuino," *Precision Microdrives*, 16-May-2016.[Online].Available: https://www.precisionmicrodrives.com/tech-blog/2016/05/16/how-drive-vibration-motor-arduino-and-genuino. [Accessed: 07-Apr-2017].

[7] "TDC7200 Evaluation Module," *TDC7200 Evaluation Module - TDC7200EVM - TI Tool Folder*. [Online]. Available: http://www.ti.com/tool/tdc7200evm. [Accessed: 06-Nov-2016].

[8] 2009 U. J. 11, "Tennessee Council of The Blind," *The History of the White Cane*. [Online]. Available: http://www.acb.org/tennessee/white_cane_history.html. [Accessed: 07-Apr-2017].

[9]"Vibration Motors," *Precision Microdrives*. [Online]. Available:https://www.precisionmicrodrives.com/vibration-motors. [Accessed: 07-Apr-2017].

ENGINEERS

WILFREDO ORTIZ

Wilfredo is an undergraduate student pursuing a BS in Photonic Science and Engineering and is set to graduate in May 2017. He has spent the last year and a half in the UCF/Lockheed Martin College Work Experience Program working with electro-optical devices and would like to continue working with lasers, electro-optics, and imaging systems.

HENRY SCHMITZ

Henry is a senior Electrical Engineering student and will be graduating Spring 2017 from the University of Central Florida. He is currently pursuing a career in the energy field, with strong interests in renewable energy and power systems.

JOSEPH DEVENPORT

Joseph is a Photonic Science and Engineering student at the University of Central Florida. Joseph intends to develop a career in the photonics engineering industry.

CEDRIC HARPER

Cedric Harper is a senior majoring in Electrical Engineering at the University of Central Florida. He plans on graduating May 2017. With a keen interest in embedded design, he plans on entering a related field.